Cre/*lox*-mediated chromosomal integration of biosynthetic gene clusters for heterologous expression in *Aspergillus nidulans*

Indra Roux [1], Yit-Heng Chooi [1]

[1] School of Molecular Sciences, University of Western Australia, Perth, WA 6009, Australia.

Correspondence to: yitheng.chooi@uwa.edu.au

Abstract

Building strains of filamentous fungi for stable long-term heterologous expression of large biosynthetic pathways is limited by the low transformation efficiency or genetic stability of current methods. Here, we developed a system for targeted chromosomal integration of large biosynthetic gene clusters in *Aspergillus nidulans* based on site-specific recombinase-mediated cassette exchange. We built *A. nidulans* strains harbouring a chromosomal landing pad for Cre/*lox*-mediated recombination and demonstrated efficient targeted integration of a 21.5 kb heterologous region in a single step. We further evaluated the integration at two loci by analysing the expression of a fluorescent reporter and the production of a heterologous polyketide. We compared chromosomal expression at those landing loci to episomal AMA1-based expression, which also shed light on uncharacterised aspects of episomal expression in filamentous fungi. This is the first demonstration of site-specific recombinase-mediated integration in filamentous fungi, setting the foundations for the further development of this tool.

Keywords: biosynthetic gene clusters, Cre/*loxP*, heterologous expression, filamentous fungi, natural product

Introduction

Filamentous fungi are prolific producers of enzymes and bioactive metabolites with biotechnological applications in pharmaceutical, agricultural and food industries.[1,2] Importantly, fungal secondary metabolites (SMs) remain a promising source of novel drug leads.[3] The genes required to produce a SM are usually colocalised in the genome forming biosynthetic gene clusters (BGCs).[3] Each BGC contains around 2–20 genes including a large backbone enzyme, such as a polyketide synthase (PKS) or a non-ribosomal peptide synthetase. BGCs can be easily identified in fungal genomic information and uncharacterised BGCs represent an almost untapped resource for compound discovery. However, a large fraction of BGCs remain silent or lowly expressed under standard culture conditions, which

limits their analysis.[3] Additionally, as novel BGCs are often found in fungal species that are difficult to cultivate or genetically intractable, heterologous expression in hosts with more genetic tools available is preferred for compound elucidation.[4]

Filamentous fungi hosts present several advantages for the heterologous expression of BGCs from other filamentous fungi, such as increased compatibility of promoters and intron splicing, and their natural capability for producing SMs.[4–6] In particular, *Aspergillus nidulans* has been widely used to produce SMs by chromosomal integration or episomal expression of heterologous BGCs.[6] Episomal systems based on the replicator AMA1 have facilitated initial testing of BGC products due to their high transformation efficiency compared to integrative vectors.[7–9] However, the phenotypic stability of AMA1-vectors has been shown to be limiting, even under selective conditions.[10] Therefore, chromosomal expression is preferred for large-scale long-term stable bioproduction in industrial settings.[11] Additionally, strains with chromosomally encoded genes can be grown in low-cost complex substrates,[12] as they do not require maintaining selection pressures.

Currently, targeted chromosomal integration in *A. nidulans* is pursued through homologous recombination (HR) facilitated by strains deficient in the non-homologous end joining pathway (*nkuA*Δ).[13] However, HR efficiency drops when integrating large constructs.[11] As a result, HR-mediated integration of large BGCs relies on the laborious stepwise integration of smaller BGC fragments.[14,15] To leverage the increasing amount of BGCs identified in novel fungi, new methods are needed for the fast creation of strains for heterologous BGC expression.[16]

Here, we develop a Cre/*lox* site-specific recombinase system for one-step chromosomal integration of BGCs in the heterologous host *A. nidulans*. Site specific recombinases are well suited for the integration of large DNA regions, as they mediate the strand exchange between the recombination sites in a size-independent manner.[17] As Cre/*loxP* recombination is reversible, strategies for irreversible integration rely on mutated *lox* sites, either on its 8-bp asymmetric core or 13-bp palindromic arms. Heteromeric *lox* sites contain nucleotide variations in the left or right arms, respectively named LE and RE.[18] LE/RE integration relies on a single recombination event between a chromosomal *lox* site and the donor vector, but results in the integration of the complete donor vector (Figure 1). Another strategy for integration relies on two sequential recombination events between two pairs of heterospecific *lox* sites (harbouring mutations in the core) named Recombinase Mediated Cassette Exchange (RMCE). In RMCE the chromosomal landing pad is flanked by two *lox* sites that are incompatible between themselves but compatible with the sites flanking the genes of interest located in the donor vector. In the presence of the Cre recombinase, the donor vector is integrated at the landing pad while in a second recombination event the donor vector

backbone and the first landing pad cassette are excised, resulting in the irreversible integration of the genes of interest (Figure 1). RMCE has been used for the integration of large constructs in a wide range of cell factories and model organisms.[19–23]

Cre/*lox*-mediated recombination has been widely used for the excision of marker genes in filamentous fungi[24–31], but there was no system for site-specific recombinase-mediated chromosomal integration in filamentous fungi. Here, we build a fungal vector set for Cre/*lox*-mediated integration and demonstrate that this tool is an efficient alternative for the integration of large heterologous BGCs in *A. nidulans*, with the potential to be expanded to other filamentous fungi.

Results

Design and construction of a recombinase-mediated integration system in *Aspergillus nidulans*

Cre/*lox*-mediated irreversible integration can be achieved by different strategies such as RMCE or LE/RE, making use of different engineered *lox* sites.[18] To simultaneously evaluate the feasibility of RMCE and LE/RE based chromosomal integration in *A. nidulans* we designed a combined strategy (Figure 1). We designed *lox* sites that contained both the heterospecific mutation of *lox2272* [32] and either of the heteromeric mutations of *lox71* and *lox66* [33], creating the sites *lox2272-71* and *lox2272-66* (Table S1). In principle, *lox2272-71* and *lox2272-66* recombination is irreversible as it results in the double LE/RE mutant site *lox2272-72* and *lox2272* (Table S1). Additionally, those sites are incompatible with *loxP* for recombination. By flanking the donor cassette and landing pad by *loxP* and either *lox2272-71 or lox2272-66,* the system can also be used for RMCE (Figure 1).

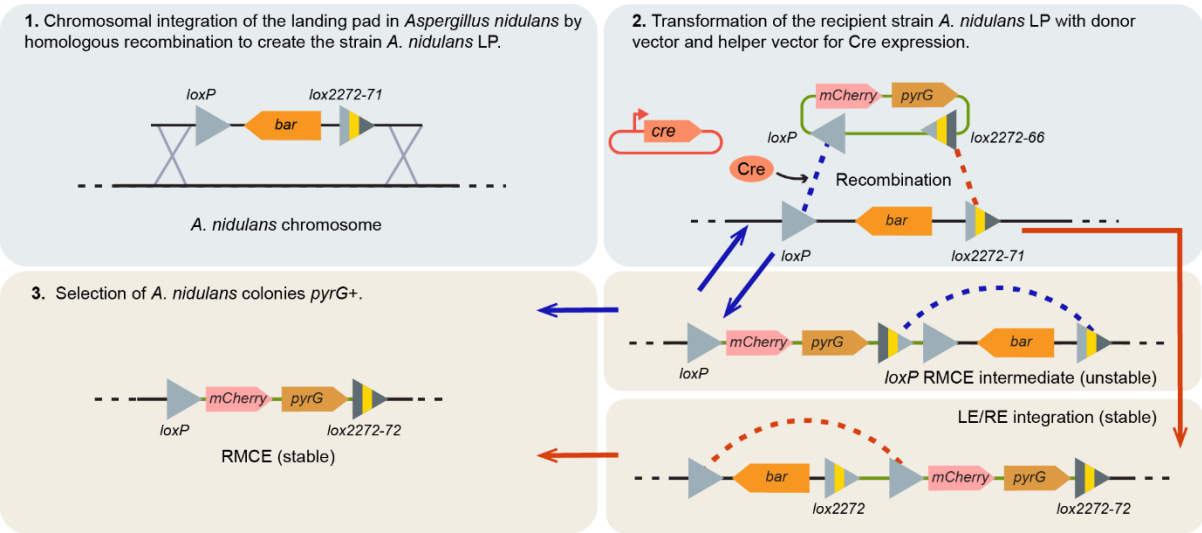

Figure 1 Overview of the strategy for Cre/*lox*-mediated chromosomal integration. **1)** The landing pad (LP) containing the *bar* marker gene flanked by *loxP* and *lox2272-71* is integrated in the destination locus of *Aspergillus nidulans* by homologous recombination.. **2)** *A. nidulans* LP protoplasts are transformed with the donor vector that contains *loxP* and *lox2272-66* flanking the marker gene *pyrG*, a fluorescent reporter and the genes of interest, along with a second vector for transient expression of *cre* recombinase. Stable integration can be achieved by LE/RE in 1-step recombination or in 2-steps by RMCE. **3)** Selection of the recombinant colonies in minimal media for *pyrG* complementation.

First, we validated the capability of Cre to recombine the sites *lox2272-66 and lox2272-71* by an assay *in vitro* (Figure S1). To create the recipient fungal strain, we chromosomally integrated the floxed (flanked by *lox* sites) landing pad (LP) by homologous recombination in the strain *A. nidulans* LO8030.[34] The landing pad consisted of the sites *loxP* and *lox2272-66* (Figure 1, Table S1) flanking the marker *bar* for glufosinate resistance. We selected as a first landing locus the sterigmatocystin (*stc*) biosynthetic gene cluster boundaries located in *A. nidulans* chromosome IV, as we previously used this locus for chromosomal expression of other genes.[35] After glufosinate selection of the transformant colonies and PCR verification, the strain *A. nidulans* landing pad 1 (LP1) was isolated for future tests.

For transient Cre recombinase expression, we created a helper vector unable to replicate in *A. nidulans.* The helper vector encodes a cassette for constitutive expression of Cre under the promoter *gpdA* (P_{gpdA}) and the terminator *trpC* (Figure 1). As the recipient strain *A. nidulans* LP1 carries *nkuA*Δ, which minimises random integration events, the helper vector presumably would be lost during fungal growth.[13]

To test the feasibility of RMCE/LE-RE integration at LP1, we built different donor vectors containing the fluorescent reporter *mCherry* and the *pyrG* marker flanked by *loxP* and *lox2272-71* (Figure 1, Figure S2A). Donor vector 1 is 6.6 kb long while donor vector 2 is a 12.2 kb shuttle vector that supports optional transformation-associated recombination cloning in *Saccharomyces cerevisiae*. Donor vector 2 also contains within the floxed region four cloning sites for the expression of biosynthetic genes under strong alcohol inducible promoters, derived from the vector pYFAC-CH2[8] (Figure S2A). As the four-promoter multiple cloning site is flanked by EcoRI sites, donor vector 2 can also be used for cloning genomic fragments containing a BGC. To demonstrate the utility of donor vector 2, we used it to clone an 18 kb region of *Aspergillus burnettii* by isothermal assembly, resulting in a 21.7 kb floxed donor region. This vector, named donor vector 2-bue contains the genes *bueA/B/C/D/E/R* responsible for the biosynthesis of preburnettiene B (**1**) [36] (Figure S2A). As burnettienes are produced in *A. burnettii* (*bue* cluster is not silent), we hypothesised that if the *bue* genes were chromosomally integrated at a good expression locus in *A. nidulans* we would observe the production of **1** as proof-of-concept (Figure S2B) [37]

Evaluation of recombination efficiency across different donor vectors

To evaluate the efficiency of the recombination system, we transformed protoplasts of *A. nidulans* LP1 by a small-scale PEG mediated transformation in 2 mL microtubes (approximately 5×10^6 protoplasts) (Figure 2A). We tested different amounts and ratios for each donor vector and the helper vector, and we also transformed the donor vector alone as a control. We consistently obtained transformant colonies in the strains cotransformed with the helper vector for *cre* expression (3–13 colonies per transformation event) (Table 1). The variation in the number of transformant colonies was independent of the size of the transformant vector, which is expected for recombinase-mediated integration (Table 1). [21]

In the control strains without *cre* helper vector we mostly observed only small "abortive" colonies that did not support further growth. Abortive colonies arising from residual non-integrated vector encoding *pyrG* have been previously reported in *A. nidulans* Δ*nkuA.*[13] Interestingly, we observed a higher number of abortive colonies when transforming the smaller donor vector 1 compared to the larger donor vector 2 and donor vector 2-*bue*. Additionally, we did not observe viable colonies in the controls when transforming the larger donor 2 and donor 2-*bue* (Table 1).

To evaluate the mechanism of integration in the transformant *pyrG*+ colonies, we analysed the landing locus by PCR amplification of the recombination junction regions (Figure 2, Figure S3). The screening strategy consisted in four PCR tests per sample, designed so one primer would bind either neighbouring region at the 5′ or 3′ from the landing locus and the other primer would bind inside of the floxed region from either the original landing pad or recombination product (Figure 2B, Figure S3A). The expected amplicon size is ~1.5 kb in all PCRs and is indicative of recombination or presence of the original landing pad for each *lox* site (Figure 2C, Figures S3C–D). We verified representative PCR amplicons by Sanger sequencing, which confirmed *in vivo* that the recombination product between *lox2272-66* or *lox2272-71* is the double LE/RE mutant site *lox2272-72* (Figure 2D).

Analysing the total of transformant colonies per experiment, the frequency of successful recombinase-mediated integration ranged 29–100% across experiments (Table 1). We observed that lower recombination efficiency was found in transformations carried out with ≤0.9 pmol of helper vector. At higher amounts of helper vector transformed (≤1.5 pmol), Cre-mediated recombination efficiency for donor vector 1 ranged 60–83% (Table 1). Importantly, the recombination efficiency of the larger vectors donor 2, and donor 2-bue ranged a 90–100% at the highest helper vector concentrations (Table 1, Figures S3C–E). The lower frequency of false positives seems to indicate that larger donor vectors are less prone to random integration.

Table 1 Cre/*lox*-mediated integration experiments in *Aspergillus nidulans*, with controls (C) and landing pad (LP) parent strain indicated.

Donor vector	LP	Transformation event	Donor (pmol[a])	Helper (pmol[a])	Colonies with Cre-mediated integration from total[b]
Donor vector 1 (6.6 kb)	LP1	1	0.63	2.41	3/5 (60%)
		2	1.10	1.67	5/6 (83%)
		3	0.37	0.83	2/7 (29%)
		C1	1.10	-	0/1 (0%)
		C2	0.37	-	0/1 (0%)
Donor vector 2 (12.2 kb)		1	0.94	1.67	12/13 (92%)
	LP1	C1	0.94	-	No colonies[c]
Donor vector 2-*bue* (27.2 kb)	LP1	1	0.53	1.67	9/9 (100%)
		2	0.64	1.67	5/5 (100%)
		3	0.64	0.33	1/3 (33%)
		C1	0.53	-	No colonies[c]
		C2	0.64	-	No colonies[c]
		C3	0.64	-	No colonies[c]
	LP2	1	0.47	2.25	4/4 (100%)
		2	0.47	2.25	3/3 (100%)
		C1	0.47	-	No colonies[c]

[a] Estimated based on vector concentration obtained by Nanodrop after standard miniprep, which might overestimate DNA concentration.
[b] Per reaction 3–6×10^6 *A. nidulans* protoplasts were used.
[c] No viable colonies. Abortive colonies were inoculated in fresh media, but no growth was observed.

When analysing the recombination outputs (RMCE, LE/RE, *loxP* intermediate), we observed variable results across experiments and donor vectors (Figure 2E, Figure S3B). Overall, around half of the colonies that recombined at LP1 presented complete RMCE (N=17), while the rest were the intermediates LE/RE (N=6) and *loxP* (N=14) (Table 1). While *loxP* recombination is reversible, in the absence of Cre recombinase activity this intermediate should be stable. When analysing all experiments by PCR for the presence of the *cre* gene we obtained PCR positive results in several colonies across experiments (Figure S4). These results could imply that random integration of the *cre* helper vector occurs in *A. nidulans* or that traces of the residual vector might be present at later growth stages.

Our screening strategy consisted in testing for the presence of recombination product along with presence or absence of the original landing pad (Figure 2A, Figure S3A). Our results seem to be indicative of genetic heterogeneity in the primary colonies, as a big proportion of transformant strains gave positive PCR results for the recombination product as well as the original landing pad (Figures S3C–E). If the first recombination event happened at a later polynuclear developmental stage the primary colonies could be heterokaryons,

requiring subsequent isolation by restreaking on selective conditions. At this stage, we decided to proceed by investigating the phenotypic stability of the transformant colonies by analysing the reporter genes.

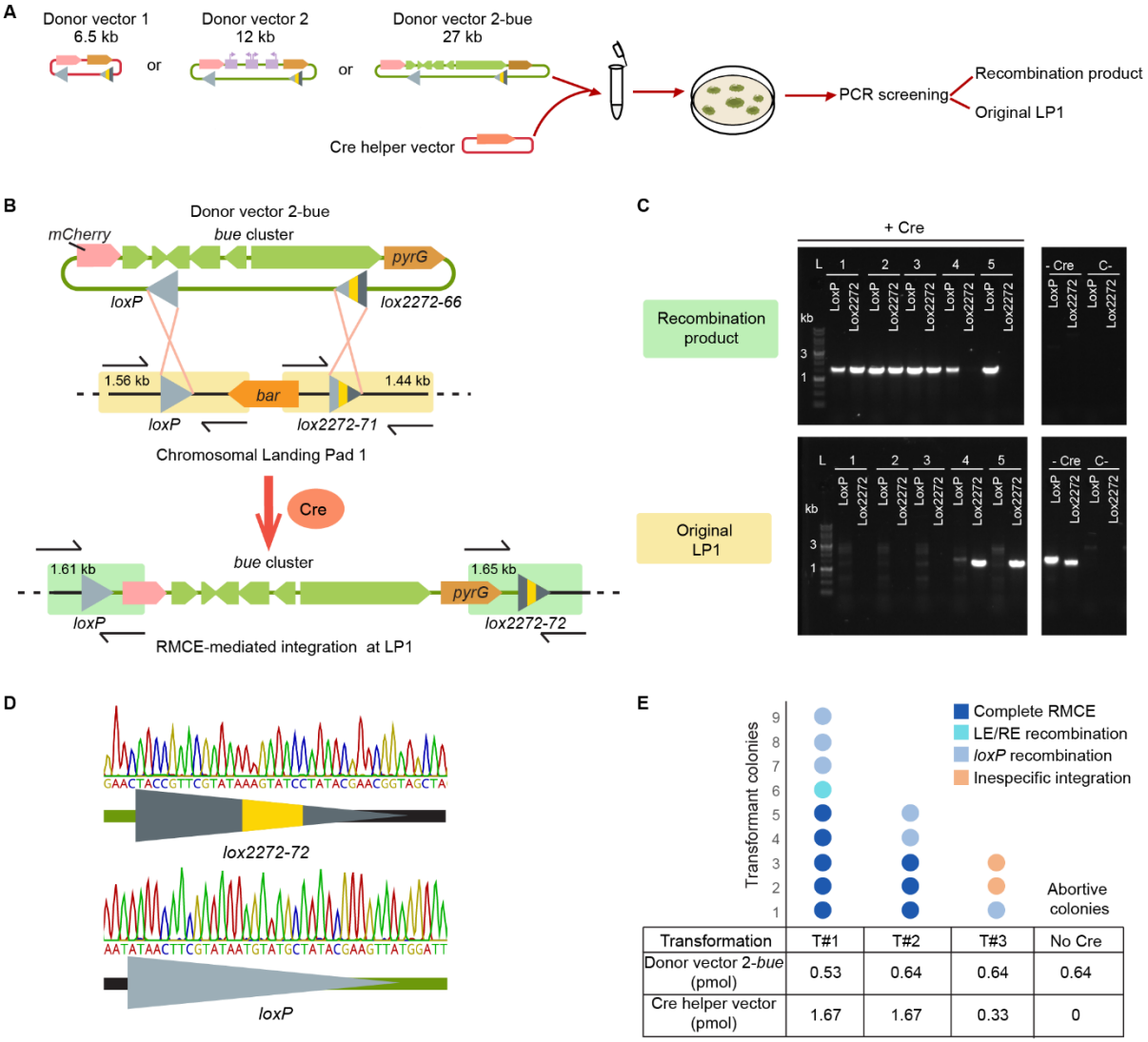

Transformation	T#1	T#2	T#3	No Cre
Donor vector 2-*bue* (pmol)	0.53	0.64	0.64	0.64
Cre helper vector (pmol)	1.67	1.67	0.33	0

Figure 2. Efficient targeted chromosomal integration of the *bue* biosynthetic gene cluster in *Aspergillus nidulans* **A.** Experimental setup for the evaluation of donor vectors. **B.** Schematic the strategy for *bue* cluster genes integration at landing pad 1 (LP1). Primer binding sites and PCR regions used for screening are indicated in the scheme with the amplicon sizes indicated. **C.** Representative PCR results of transformant colonies for donor vector 2-*bue* integration. Colonies are indicated as numbers, and the complete gel is found in Figure S3. **D.** Confirmation of the expected recombination event by Sanger sequencing **E.** Amount of transformant colonies obtained in different transformation experiments with donor 2-bue, with the integration mechanism indicated as a colour code. Recombination is obtained across a different amount and proportion of donor vector and Cre helper vector.

Evaluating expression at landing pad 1 with a fluorescent reporter and metabolite production

To evaluate the strains with recombinase-mediated integration at LP1, we first analysed the expression of the fluorescent reporter mCherry encoded in the donor cassette. To benchmark chromosomal expression at LP1, we compared this expression system to strains expressing mCherry from episomal AMA1-pyrG vectors. We consistently observed fluorescence in mycelia of colonies with mCherry integrated at LP1 compared to the negative control (Figure 3A, Figure S5). However, fluorescence in strains with mCherry integrated at LP1 was low compared to the AMA1-encoded counterpart under selective conditions. We also observed that when hyphae from strains harbouring AMA1-pyrG encoded P_{gpdA}-*mCherry* were grown in non-selective conditions, some hyphae retained higher fluorescence than their LP1-integrated counterpart (Figure 3A, Figure S5).

Inspired by comparative studies of chromosomal and episomal expression in yeast by Jensen *et al,*[38] we analysed the spores of recombinant colonies by flow cytometry to test phenotypic stability. We observed a unimodal distribution of fluorescence in the strains with *mCherry* integrated at LP1, distinguishable from the negative control (Figure S6A). The strains with AMA1-based episomal expression of *mCherry* presented a much wider multimodal distribution (Figure S6A), which is expected due to the phenotypic instability of AMA1-encoded genes on spores even under selective conditions.[10] While these results indicated that chromosomal expression at LP1 results in a more homogeneous cell population, expression at LP1 is at least one order of magnitude below the signal from the best performer spores of AMA1-episomal expression. Overall, our analysis of the fluorescent reporter at LP1 by flow cytometry and microscopy supported phenotypic stability, which is expected of chromosomally integrated genes.

To assess compound production at LP1, we cultivated different transformant strains of Cre/*lox*-mediated integration of donor vector 2-*bue* (N=9) (Figure S7). However, we did not observe detectable compound production when the genes were integrated at LP1, while we consistently observed production of **1** in the strains with episomal expression (N=8) (Figure S7).

Overall, when evaluating fluorescent reporter mCherry and **1**, expression at LP1 was lower than its episomal counterpart. Furthermore, the lack of compound production at LP1 makes it not an ideal locus for BGC expression for natural product discovery. To make our recombinase-mediated integration system more useful, we decided to evaluate integration at a landing locus previously validated for the production of heterologous compounds.

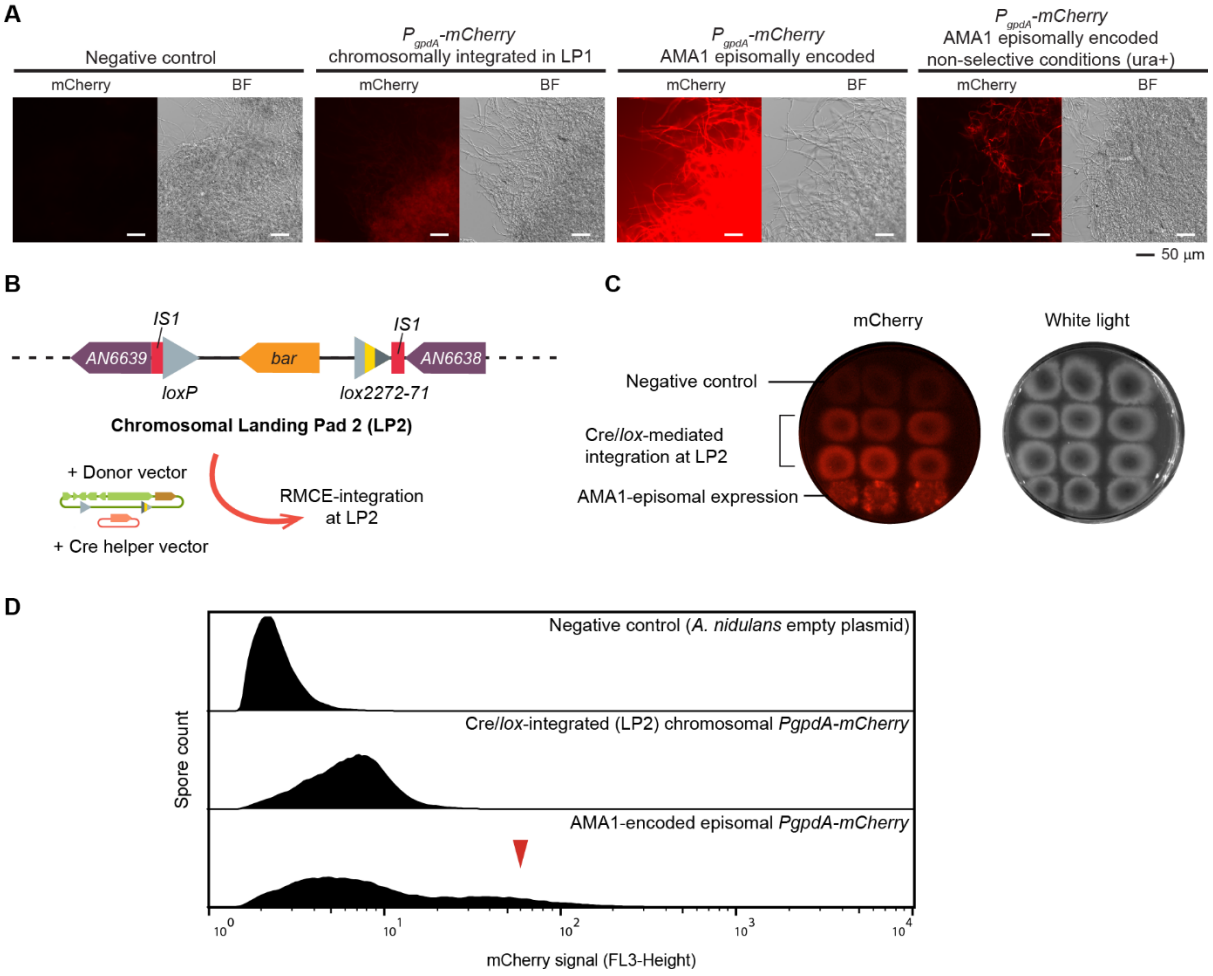

Figure 3. Chromosomal expression of mCherry at landing pads (LPs)compared to AMA1-based episomal expression. **A.** Strains with *mCherry* chromosomally integrated at LP1 show lower fluorescence than the AMA1-based episomal counterpart under selective conditions. Selection pressure is needed to support high AMA1-based episomal expression. Samples with similar mycelial growth were observed under mCherry filter and brightfield (BF) by fluorescence microscopy. Biological replicates are found in Figure S5. **B.** Overview of the strategy to evaluate the site LP2 at *Aspergillus nidulans IS1* locus. **C.** Analysis of transformant colonies by fluorescence photography shows a patchy pattern in the fluorescence of colonies with AMA1-based expression under selective conditions, compared to more homogeneous fluorescence in strains with chromosomal expression at LP2. Extended information in Figure S9. **D**. Analysis of spores by flow cytometry shows more compact and homogeneous fluorescence in samples with chromosomal integration of *mCherry* at LP2 compared to AMA1-based episomal expression. A proportion of the spores expressing mCherry episomally from AMA1 vectors can reach fluorescence levels one order of magnitude higher than spores with chromosomal expression at LP2 (see red arrow). Extended information in Figure S6.

Construction and evaluation of landing pad 2

The site *IS1* located in *A. nidulans* chromosome I has been used as a target for integration of heterologous biosynthetic genes by homologous recombination, for example the geodin BGC.[14] We proceeded to integrate our floxed landing pad at *IS1* by HR, creating the strain *A. nidulans* LP2 (Figure 3B, Figure S7A). Next, we evaluated recombinase-mediated

integration at LP2 of Donor vector 2-*bue* (Figure S7). In both transformations tested we obtained 100% efficiency of recombinase-mediated integration, with complete or intermediate RMCE, as evaluated by diagnostic PCR (Table 1, Figure S7B–C).

At this stage, we also evaluated the use of a replicative AMA1-based vector containing the floxed *pyrG* cassette as donor vector 3 (Figure S8). However, we did not obtain evidence of recombination with this prototype, which highlights the relevance of selecting for the recombination event and not just DNA uptake (Figure S8).

To evaluate the expression of genes integrated at LP2, we first assessed the fluorescent reporter mCherry. Inspired by Vanegas *et al*, where an mCherry reporter integrated at *IS1* was assessed with fluorescent photography we first evaluated the transformant colonies by a similar method.[39] In our assay, we replicated transformant colonies in solid media under selective and non-selective conditions and benchmarked it against AMA1-based expression (Figure 3C, Figure S9). We observed that the strains with chromosomal integration of mCherry at LP2 showed uniform fluorescence in selective and non-selective conditions, distinguishable from the negative control. Interestingly, the strains with AMA1-encoded mCherry presented a patched expression pattern on the conidia on the colony surface with some regions displaying high fluorescence under both selective and non-selective conditions (Figure S9A). To further investigate the pattern of AMA1-based mCherry expression, we performed a spore dilution and plated under selective and non-selective conditions (Figure S9B). We observed that in non-selective supplemented media we obtained a mixture of colonies with no noticeable fluorescence along with colonies with observable patchy fluorescence. Interestingly, the colonies with fluorescence in non-selective media were comparable to the colonies under selective conditions.

To further analyse the profile of mCherry expression at LP2, we analysed spores from different transformant colonies by flow cytometry. We observed a similar pattern to the strains with mCherry integrated at LP1 (Figure 3D, Figure S6). These results indicate that P_{gpdA}-*mCherry* integrated at either LP2 or LP1, failed to achieve the fluorescence levels comparable to the best performer spores in the multicopy AMA1-encoded P_{gpdA}-*mCherry.* We also observed lower fluorescence in mycelia from strains with chromosomal expression at LP2 compared to AMA1-based episomal counterparts (Figure S5).

Next, we evaluated the production of **1** in the *A. nidulans* strains with *bue* genes integrated at LP2. After cultivation, like the strains with *bue* genes integrated at LP1, we did not observe the production of **1** in the recombinant strains (N=5) when analysing media extracts (Figure S10A). For troubleshooting, we verified that the end of culture fungal pellets expressed mCherry (Figure S10A). As a next troubleshooting step, we investigated two

transformant strains with *bue* genes integrated at LP2 and one at LP1 by whole genome sequencing (Figure S11). We confirmed the expected recombination with no mutations that could explain the lack of compound production. Thus, the lack of compound production could be due to the *bue* genes being silent when integrated chromosomally.

Activation of chromosomally integrated *bue* genes by transcription factor overexpression

As the strains with chromosomal integration of *bue* genes at LP1 or LP2 did not produce compound **1**, we hypothesised that overexpression of the *bue* cluster-specific transcription factor (TF) *bueR* could activate the cluster in chromosomal context.

For each landing locus, we selected a representative transformant strain with the *bue* genes integrated by RMCE and prepared protoplasts (Figure 4B,C). After transformation with the vector *pYFAC-*P_{gpdA}*-bueR-bueG (Ref),* we observed that the strains overexpressing the TF BueR presented production of compound **1**, while the control strains with an empty vector did not present compound production (Figure 4). This result validates that the strains had integrated a functional and complete copy of the *bueA/B/C/D/E/R*. When comparing the strains with *bue* genes integrated at LP1 and LP2, we observed similar production levels between them (Figure 4C).

One of the benefits of chromosomal expression is that cultures can be grown under non-selective conditions without compromising productivity. For simplicity, in previous small-scale culturing experiments we cultivated the strains on liquid minimal media with no uracil and uridine, the selective condition of the *pyrG* marker. To evaluate expression under non-selective conditions, we cultivated replicates from the strains containing the *bue* genes at LP2 and TF overexpression in media supplemented with uracil and uridine. It should be noted that the AMA1-based vector for TF expression is under the selection of pyridoxal auxotrophy with the *pyroA* marker and the medium used lack pyridoxine. As expected, the uracil and uridine selection pressure was not needed for compound production (Figure 4B). Interestingly, we observed a 3-fold higher production in the strains grown in non-selective conditions (Figure 4C). Positional effects arising for insufficient expression of the *pyrG* marker integrated in some loci have been observed in *A. nidulans* before, however changes in compound production in uracil/uridine supplemented media could be due to other effects.[40,41]

To sum up, overexpression of the cluster-specific TF allowed to activate the expression of *bue* genes at two different chromosomal contexts. These results demonstrate that recombinase-mediated integration is a feasible strategy to build strains for heterologous compound production, but that alternative strategies might be needed for BGC activation it the

cluster remains silent. Overall, chromosomal expression permitted cultivating in non-selective media without compromising yields.

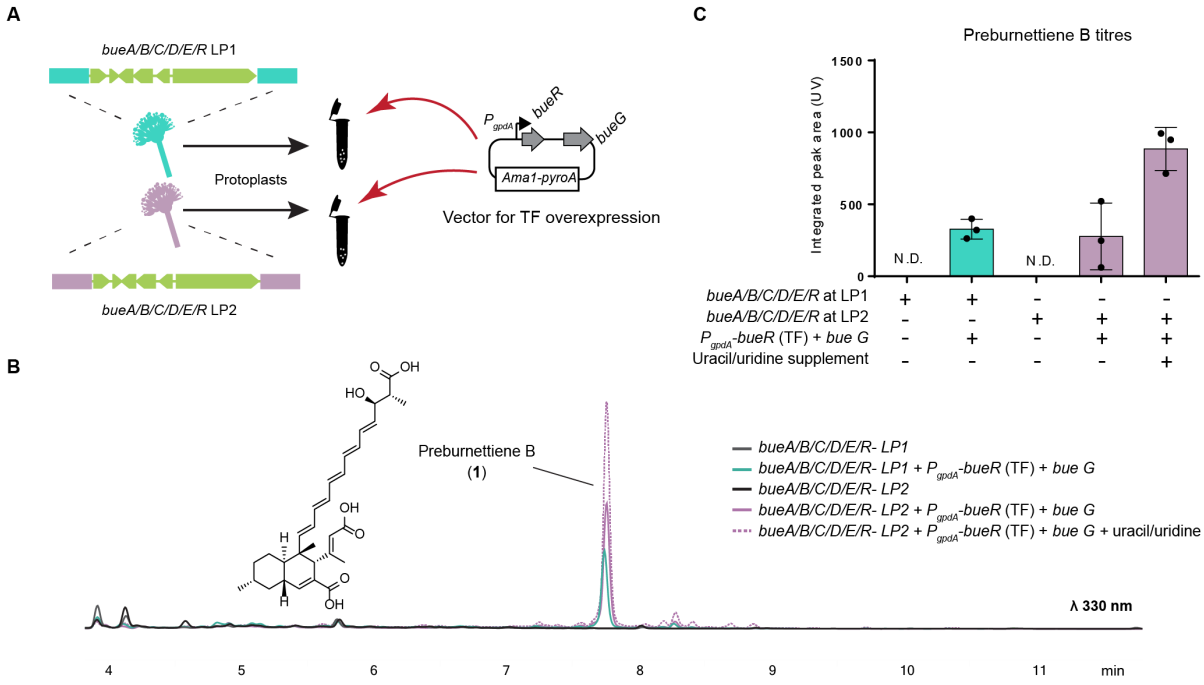

Figure 4. Activation of chromosomally integrated *bue* cluster genes by transcription factor (TF) overexpression. **A.** Protoplasts were prepared from strains with RMCE integrated *bue* genes at LP1 or LP2, and further transformed with a vector containing the construct P_{gpdA}-*bueR* TF overexpression and *bueG* encoding a transporter. **B.** Chromatogram traces at 330 nm show activation of preburnettiene B (**1**) production on strains with TF overexpression. **C.** Quantification of the production of **1** show comparable compound levels in the strains with the genes integrated at LP1 or LP2 with TF overexpression on minimal media. Strains grown on media supplemented with uracil and uridine (non-selective condition) presented higher titres than the same strain grown on minimal media (selective condition). Calculated integrated peak area values are the mean of three biological replicates, specific values are indicated as black dots, and error bars represent SD. Two-sided Welch's T-test p-value ≥ 0.024 .

Discussion

In this work we established a system for Cre/*lox*-mediated chromosomal integration of large heterologous BGCs in *A. nidulans*. Site-specific recombinase mediated integration represents a relevant expansion to the synthetic biology toolbox for filamentous fungi, where recombinases had only been used for gene deletion or inversion.[31] The vector set developed in this work has the potential to be easily adapted for integration at different chromosomal landing loci or related fungal chassis.[42]

We demonstrated targeted one-step integration of long DNA regions of up to 27 kb by LE/RE and 21 kb by RMCE in *A. nidulans*. We obtained high transformation efficiency (up to 100%) using a small-scale transformation protocol with optimised amounts of helper vector.

We additionally observed that the false positive rate and the presence of abortive colonies diminished when transforming large donor vectors (≥12 kb). We also demonstrated that the resulting strains with chromosomally encoded genes presented a more uniform fluorescence phenotype in spores and mycelia compared to AMA1-encoded genes, evidencing genetic and phenotypic stability.

The developed Cre/*lox*-mediated integration system presents an advantageous alternative to HR for the single-step integration of large DNA constructs. However, it also faces the same constraints as HR for heterologous expression featuring a single gene copy in a chromosomal context. When integrating the heterologous genes *bueA/B/C/D/E/F/R* under their native promoter at LP1 or LP2 initially we did not observe compound production, unlike the episomal counterpart. Nevertheless, when overexpressing the cluster specific TF *bueR* we restored compound production from biosynthetic genes at LP1 and LP2. Strategies for BGC activation, such as TF overexpression, promoter replacement or CRISPRa could be used to activate chromosomally integrated genes that remain silent.[35] Alternatively, integration in a better locus for expression could also result in improved performance.

By benchmarking chromosomal expression to AMA1-*pyrG* based expression, this work also represents an unprecedented characterisation of AMA1-*pyrG* episomal expression in *A. nidulans*. We analysed episomal expression in fungal growth in both solid media and submerged liquid culture, which have different morphological and developmental characteristics. While *A. nidulans* grown in solid media completes the developmental stages that lead to sporulation, fungal growth in liquid submerged culture gets arrested in an undifferentiated hyphal state with almost no conidia production.[43,44] In the literature, AMA1 expression is usually characterised by observing the phenotype of spores grown on solid selective media.[4,10] Our original analysis of AMA1-pyrG phenotypic stability by flow cytometry adds a quantitative estimation of the phenotypic heterogeneity of AMA1-based expression in spores from in *A. nidulans* grown under selective conditions in solid media. This is particularly relevant considering the impact of spore expression in fungal development.[45] Even though our results indicate that the phenotypic stability of AMA1-encoded genes in spores is limited, we observed that during mycelial growth in liquid culture there is a more prevalent phenotype for strong expression in both fluorescence and compound production.

Lastly, the Cre/*lox*-mediated integration platform can be expanded in future works. Cre-mediated integration could be particularly relevant for integrating large genomic regions containing BGCs cloned by genome capture.[9] The current system could also be upgraded for simultaneous integration in different loci by using multiple landing pads with different heterospecific recombination sites. Different strategies could also be evaluated to optimise the delivery of Cre recombinase, such as self-excising Cre expression cassettes.[22] The use of a

split *pyrG* marker between recombination sites could be evaluated to minimise the background by random integration and abortive colonies, or to further evaluate AMA1-based donor vectors.[46]

To sum up, Cre/*lox*-mediated integration of BGCs has the potential to speed up the process of constructing strains to produce heterologous metabolites in *A. nidulans.* The capability to uptake and maintain complex exogenous DNA is a key requirement for a good chassis organism for bioproduction.[47] Thus, this system can be used to upgrade other filamentous fungi chassis.

Methods

Vector Construction

All vectors are listed in Table S2 and the oligonucleotides used are listed in Table S4 with their destination vector indicated. Vectors were constructed by isothermal assembly or digestion with restriction site enzymes and ligation. Cloning strategies for each vector are detailed in Supporting Methods. *Cre* was amplified from pBF3038.[48] Relevant vectors will be made available via Addgene (Table S2).

Aspergillus nidulans strains construction and transformation

Genotype of parental strains are listed in Table S3. *A. nidulans* parental strains with LP1 or LP2 were created by polyethylene glycol (PEG)-calcium-based transformation [49] with NotI linearized vectors pGemLP1-loxP-bar-Lox2272-71 or pGemLP2-loxP-bar-Lox2272-71 containing 1 kb homology regions for homologous recombination in *A. nidulans* LO8030. Colonies were selected for resistance to glufosinate extracted from Basta, as previously[35], an the event was confirmed by diagnostic PCR.

Protoplasts of *A. nidulans* LO8030 LP1 or LP2 were prepared from germlings [49], mixed with a quarter volume PEG 60% to a final concentration of 10^8 protoplasts per mL and frozen at -80 °C for later use. AMA1-vectors were transformed into *A. nidulans* protoplasts in a 2 mL microcentrifuge tube, 60 µL of thawed protoplast solution was incubated with 40 µL of STC buffer (1.2 M sorbitol, 10 mM $CaCl_2$, 10 mM Tris–HCl, pH 7.5) and the vector amounts indicated in Table 1. After 20 min of incubation on ice, 400 µL of the calcium PEG 60% mix was added and mixed gently by inversion, followed by a 20 min incubation at room temperature. After adding 1 mL of STC buffer the mix was spread on stabilised minimal media (SMM) supplemented with pyridoxine (p+) and riboflavin (r+) but lacking uracil or uridine (u-) for auxotrophic selection (u-p+r+), divided in two plates that were then incubated for three days at 37 °C to generate transformant colonies.

For the activation of the chromosomally integrated *bue* genes by TF overexpression, protoplasts were prepared from the strains *A. nidulans LO8030-LP1-bueA/B/C/D/E/R* and *A. nidulans LO8030-LP2-bueA/B/C/D/E/R.* Protoplasts were transformed with the vector pYFAC-bueG-PgpdA-bueR[36] and selected on SMM u-r+p-.

Relevant strains were analysed by whole genome sequencing with the DNBSEQ-2000 PE150 platform at BGI Tech Solutions co. (BGI, Hong Kong), resulting in ~2 Gb of raw genome data (150 bp, paired-end). The reads were mapped to chromosome sequences containing the expected recombination product using Geneious 11.03.

Diagnostic PCRs

Genomic DNA (gDNA) was extracted from mycelial mass after overnight growth in liquid glucose minimal media (GMM) u-p+r+ at 37 °C. The PCR amplification was conducted by 3 min at 94 °C initial denaturing followed by 27 cycles of 30 s at 94 °C, 30 s at 56.5 °C, 60 s at 72 °C, in a thermocycler with Taq polymerase, using ~30 ng of *A. nidulans* gDNA in a 10 µl reaction volume. The PCR products were run in a 0.8% agarose gel with 2 µl of the AccuRuler 1 kb DNA RTU Ladder (Maestrogen). All agarose gel images were acquired with a Vilber E-Box VX-2 gel imager. Representative PCRs products were amplified with Pfu polymerase for Sanger sequencing.

Fluorescence microscopy

Spores from three or more individual colonies were picked and grown overnight at 37° C in small petri dishes containing liquid GMM u-p+r+ or u+p+r+. Fluorescence images were captured at 20x on the epifluorescence inverted microscope Eclipse Ti2 (Nikon), using numerical aperture (NA) 0.75 and Plan Apo λ 20x objective lens (Nikon) and a Camera DS-Qi2 (Nikon) controlled by NIS Elements Advanced Research (Nikon). Fluorescent microscopy was carried out under a mCherry filter set (562/40 nm excitation, 593 nm dichroic beamsplitter, and 641/75 nm emission), using a 400 ms exposure and 1.8x analog gain unless specified otherwise. Images were recorded using NIS-Elements Advanced Research software package (Nikon).

Flow cytometry

Spores were collected in water with a sterile loop from colonies grown for 3 days in solid GMM u-p+r+ r. The spore suspension was filtered through a syringe containing sterile cotton to remove residual mycelia and diluted to a concentration of ~1.10^6 spores/mL. Data acquisition was performed immediately after spore suspension using a FACSCalibur (BD Biosciences) flow cytometer operated with filtered water as shear fluid. mCherry signal was observed with a 488 nm excitation laser and the filter FL3 (≥670 nm) and 35,000 events were

detected per measurement or 4 minutes of run were collected for the water control. The data was processed using FlowJo V10 software (TreeStar). The output was gated according to FCS size to limit to the size range of spores, an example of the gating strategy is indicated on the Figure S6.

Fluorescent photography

Plates were analysed in ChemiDoc MP Imaging System (Bio-Rad) and images recorded with ImageLab software (Bio-Rad). MCherry images were obtained using the excitation source Green epi illumination and the emission filter 605/50 nm with exposure time of 0.01 seconds. Bright field was captured with white illumination and a standard emission filter in automatic exposure.

Metabolic profile analysis by LC-DAD-MS

For each transformant strain, spores from individual colonies were re-streaked individually in a solidified GMM (u-p+r+ or u-p-r+) plate and cultivated for three days at 37 °C. Spores were harvested from plates in 1 mL of 0.1% Tween 80 (Sigma, MO, USA) and approximately 10^8 spores were inoculated into 250-mL flasks containing 50 mL liquid GMM (u-p+r+, u-p-r+ or u+p-r+) medium. Additionally, ampicillin was added to 50 µg mL^{-1}. Cultures were incubated for 4 days with shaking set to 200 rpm and 26 °C. At the end of the culture, 20 mL of media was collected in 50-mL falcon tubes by filtration with Miracloth (Milipore, MA, USA). The metabolites were extracted from the liquid culture with 20 mL of an organic solvent mixture containing ethyl acetate, methanol, and acetic acid (89.5 : 10 : 0.5 ratio). The crude extracts were dried down in vacuo and re-dissolved in 0.3 mL of methanol for LC-DAD-MS analysis.

The analyses of the metabolite profiles were performed on an Agilent 1260 liquid chromatography (LC) system coupled to a diode array detector (DAD) and an Agilent 6130 Quadrupole mass spectrometer (MS) with an electrospray ionization (ESI) source. In all cases 3 µL of the methanol dissolved crude extract was injected. Chromatographic separation was performed at 40 °C using a Kinetex C18 column (2.6 µm, 2.1 mm i.d. x 100 mm; Phenomenex). Chromatographic separation was achieved with a linear gradient of 5–95% acetonitrile-water (containing 0.1% v/v formic acid) in 10 minutes followed by 95% acetonitrile for 3 minutes, with a flow rate of 0.70 mL min^{-1}. The MS data were collected in the *m/z* range 100–1000 in negative ion mode and UV observed at DAD λ=330 nm. Peak areas were determined by peak integration of DAD λ=330 nm chromatogram using Masshunter Workstation Qualitative Analysis (Agilent). Statistical analysis was performed with GraphPad Prism 8.3.0 by a Two-sided Welch's T-test using biological triplicates.

Abbreviations

BGCs, biosynthetic gene clusters; HR, homologous recombination; LE/RE, Left/Right recombination; LP, landing pad; PKS, polyketide synthase; RMCE, Recombinase Mediated Cassette Exchange; SM, secondary metabolite.

Acknowledgments

Y.H.C. and this project is supported by an ARC Future Fellowship (FT160100233). I.R. was recipient of an UWA PhD Scholarship. This research was funded, in part, by the Cooperative Research 418 Centres Projects scheme (CRCPFIVE000119). *Aspergillus burnettii* MST-FP2249 is a gift from Microbial Screening Technologies (MST) and *A. nidulans* LO8030 is a gift from Berl Oakley. We thank Hamideh Rezaee for her help building donor vector 2, and Julia Grassl (UWA) for helping us to set up the flow cytometer. We also thank members of Lister Lab (UWA), specifically Jahnvi Pflüger, for whole plasmid sequencing.

Conflicts of interest

There are no conflicts to declare.

Author contribution

I.R and Y.H.C conceived the project and wrote the manuscript. I.R. designed and performed the experiments and the data analysis.

References

(1) Wakai, S., Arazoe, T., Ogino, C., and Kondo, A. (2017) Future insights in fungal metabolic engineering. *Bioresour. Technol. 245*, 1314–1326.

(2) Meyer, V., Basenko, E. Y., Benz, J. P., Braus, G. H., Caddick, M. X., Csukai, M., de Vries, R. P., Endy, D., Frisvad, J. C., Gunde-Cimerman, N., Haarmann, T., Hadar, Y., Hansen, K., Johnson, R. I., Keller, N. P., Kraševec, N., Mortensen, U. H., Perez, R., Ram, A. F. J., Record, E., Ross, P., Shapaval, V., Steiniger, C., van den Brink, H., van Munster, J., Yarden, O., and Wösten, H. A. B. (2020) Growing a circular economy with fungal biotechnology: a white paper. *Fungal Biol. Biotechnol. 7*, 5.

(3) Keller, N. P. (2019) Fungal secondary metabolism: regulation, function and drug discovery. *Nat. Rev. Microbiol. 17*, 167–180.

(4) Anyaogu, D. C., and Mortensen, U. H. (2015) Heterologous production of fungal secondary metabolites in Aspergilli. *Front. Microbiol. 6*, 77.

(5) He, Y., Wang, B., Chen, W., Cox, R. J., He, J., and Chen, F. (2018) Recent advances in reconstructing microbial secondary metabolites biosynthesis in *Aspergillus* spp. *Biotechnol. Adv. 36*, 739–783.

(6) Caesar, L. K., Kelleher, N. L., and Keller, N. P. (2020) In the fungus where it happens: history and future propelling *Aspergillus nidulans* as the archetype of natural products research. *Fungal Genet. Biol. 144*, 103477.

(7) Liu, L., Tang, M.-C., and Tang, Y. (2019) Fungal Highly Reducing Polyketide Synthases Biosynthesize Salicylaldehydes that are Precursors to Epoxycyclohexenol Natural Products. *J. Am. Chem. Soc. 141*, 19538–19541.

(8) Hu, J., Sarrami, F., Li, H., Zhang, G., Stubbs, K. A., Lacey, E., Stewart, S. G., Karton, A., Piggott, A. M. M., and Chooi, Y.-H. H. (2019) Heterologous biosynthesis of elsinochrome A sheds light on the formation of the photosensitive perylenequinone system. *Chem. Sci. 10*, 1457–1465.

(9) Clevenger, K. D., Bok, J. W., Ye, R., Miley, G. P., Verdan, M. H., Velk, T., Chen, C., Yang, K. H., Robey, M. T., Gao, P., Lamprecht, M., Thomas, P. M., Islam, M. N., Palmer, J. M., Wu, C. C., Keller, N. P., and Kelleher, N. L. (2017) A scalable platform to identify fungal secondary metabolites and their gene clusters. *Nat. Chem. Biol. 13*, 895–901.

(10) Aleksenko, A., and Clutterbuck, A. J. (1997) Autonomous plasmid replication in *Aspergillus nidulans* : AMA1 and MATE elements. *Fungal Genet. Biol. 21*, 373–387.

(11) Li, L., Liu, X., Wei, K., Lu, Y., and Jiang, W. (2019) Synthetic biology approaches for chromosomal integration of genes and pathways in industrial microbial systems. *Biotechnol. Adv. 37*, 730–745.

(12) Ferreira, J. A., Mahboubi, A., Lennartsson, P. R., and Taherzadeh, M. J. (2016) Waste biorefineries using filamentous ascomycetes fungi : Present status and future prospects. *Bioresour. Technol. 215*, 334–345.

(13) Nayak, T., Szewczyk, E., Oakley, C. E., Osmani, A., Ukil, L., Murray, S. L., Hynes, M. J., Osmani, S. A., and Oakley, B. R. (2006) A versatile and efficient gene-targeting system for *Aspergillus nidulans*. *Genetics 172*, 1557–1566.

(14) Nielsen, M. T., Nielsen, J. B., Anyaogu, D. C., Holm, D. K., Nielsen, K. F., Larsen, T. O., and Mortensen, U. H. (2013) Heterologous Reconstitution of the Intact Geodin Gene Cluster in *Aspergillus nidulans* through a Simple and Versatile PCR Based Approach. *PLoS*

One 8, e72871.

(15) Yin, W. B., Chooi, Y. H., Smith, A. R., Cacho, R. A., Hu, Y., White, T. C., and Tang, Y. (2013) Discovery of cryptic polyketide metabolites from dermatophytes using heterologous expression in *Aspergillus nidulans*. *ACS Synth. Biol. 2*, 629–634.

(16) Robey, M. T., Caesar, L. K., Drott, M. T., Keller, N. P., and Kelleher, N. L. (2021) An interpreted atlas of biosynthetic gene clusters from 1,000 fungal genomes. *Proc. Natl. Acad. Sci. 118*, e2020230118.

(17) Olorunniji, F. J., Rosser, S. J., and Stark, W. M. (2016) Site-specific recombinases: molecular machines for the Genetic Revolution. *Biochem. J. 473*, 673–684.

(18) Hirano, N., Muroi, T., Takahashi, H., and Haruki, M. (2011) Site-specific recombinases as tools for heterologous gene integration. *Appl. Microbiol. Biotechnol. 92*, 227–239.

(19) Santos, C. N. S., Regitsky, D. D., and Yoshikuni, Y. (2013) Implementation of stable and complex biological systems through recombinase-assisted genome engineering. *Nat. Commun. 4*, 2503.

(20) Wallace, H. A. C., Marques-Kranc, F., Richardson, M., Luna-Crespo, F., Sharpe, J. A., Hughes, J., Wood, W. G., Higgs, D. R., and Smith, A. J. H. (2007) Manipulating the Mouse Genome to Engineer Precise Functional Syntenic Replacements with Human Sequence. *Cell 128*, 197–209.

(21) Wang, G., Zhao, Z., Ke, J., Engel, Y., Shi, Y.-M., Robinson, D., Bingol, K., Zhang, Z., Bowen, B., Louie, K., Wang, B., Evans, R., Miyamoto, Y., Cheng, K., Kosina, S., De Raad, M., Silva, L., Luhrs, A., Lubbe, A., Hoyt, D. W., Francavilla, C., Otani, H., Deutsch, S., Washton, N. M., Rubin, E. M., Mouncey, N. J., Visel, A., Northen, T., Cheng, J.-F., Bode, H. B., and Yoshikuni, Y. (2019) CRAGE enables rapid activation of biosynthetic gene clusters in undomesticated bacteria. *Nat. Microbiol. 4*, 2498–2510.

(22) Garcia-Morales, L., Ruiz, E., Gourgues, G., Rideau, F., Piñero-Lambea, C., Lluch-Senar, M., Blanchard, A., and Lartigue, C. (2020) A RAGE Based Strategy for the Genome Engineering of the Human Respiratory Pathogen *Mycoplasma pneumoniae*. *ACS Synth. Biol. 9*, 2737–2748.

(23) Baer, A., and Bode, J. (2001) Coping with kinetic and thermodynamic barriers: RMCE, an efficient strategy for the targeted integration of transgenes. *Curr. Opin. Biotechnol. 12*, 473–480.

(24) Forment, J. V., Ramón, D., and MacCabe, A. P. (2006) Consecutive gene deletions

in *Aspergillus nidulans*: Application of the Cre/loxP system. *Curr. Genet. 50*, 217–224.

(25) Krappmann, S., Bayram, Ö., and Braus, G. H. (2005) Deletion and allelic exchange of the *Aspergillus fumigatus veA* locus via a novel recyclable marker module. *Eukaryot. Cell 4*, 1298–1307.

(26) Mizutani, O., Masaki, K., Gomi, K., and Iefuji, H. (2012) Modified Cre-loxP recombination in *Aspergillus oryzae* by direct introduction of Cre recombinase for marker gene rescue. *Appl. Environ. Microbiol. 78*, 4126–4133.

(27) Steiger, M. G., Vitikainen, M., Uskonen, P., Brunner, K., Adam, G., Pakula, T., Penttilä, M., Saloheimo, M., MacH, R. L., and Mach-Aigner, A. R. (2011) Transformation system for *Hypocrea jecorina* (*Trichoderma reesei*) that favors homologous integration and employs reusable bidirectionally selectable markers. *Appl. Environ. Microbiol. 77*, 114–121.

(28) Honda, S., and Selker, E. U. (2009) Tools for Fungal Proteomics: Multifunctional *Neurospora* Vectors for Gene Replacement, Protein Expression and Protein Purification. *Genetics 182*, 11–23.

(29) Florea, S., Andreeva, K., Machado, C., Mirabito, P. M., and Schardl, C. L. (2009) Elimination of marker genes from transformed filamentous fungi by unselected transient transfection with a Cre-expressing plasmid. *Fungal Genet. Biol. 46*, 721–730.

(30) Jiang, B., Zhang, R., Feng, D., Wang, F., Liu, K., Jiang, Y., Niu, K., Yuan, Q., Wang, M., Wang, H., Zhang, Y., and Fang, X. (2016) A tet-on and Cre-*loxP* based genetic engineering system for convenient recycling of selection markers in *Penicillium oxalicum*. *Front. Microbiol. 7*, 485.

(31) Krappmann, S. (2014) Genetic surgery in fungi: Employing site-specific recombinases for genome manipulation. *Appl. Microbiol. Biotechnol. 98*, 1971–1982.

(32) Lee, G., and Saito, I. (1998) Role of nucleotide sequences of *loxP* spacer region in Cre-mediated recombination. *Gene 216*, 55–65.

(33) Albert, H., Dale, E. C., Lee, E., and Ow, D. W. (1995) Site-specific integration of DNA into wild-type and mutant lox sites placed in the plant genome. *Plant J. 7*, 649–659.

(34) Chiang, Y. M., Ahuja, M., Oakley, C. E., Entwistle, R., Asokan, A., Zutz, C., Wang, C. C. C., and Oakley, B. R. (2016) Development of Genetic Dereplication Strains in *Aspergillus nidulans* Results in the Discovery of Aspercryptin. *Angew. Chemie - Int. Ed. 55*, 1662–1665.

(35) Roux, I., Woodcraft, C., Hu, J., Wolters, R., Gilchrist, C. L. M., and Chooi, Y. H. (2020) CRISPR-Mediated Activation of Biosynthetic Gene Clusters for Bioactive Molecule Discovery in Filamentous Fungi. *ACS Synth. Biol. 9*, 1843–1854.

(36) Roux, I., Bowles, S., Kalaitzis, J. A., Vuong, D., Lacey, E., Chooi, Y. H., and Piggott, A. M. (2021) Characterisation and heterologous biosynthesis of burnettiene A, a new polyene-decalin polyketide from *Aspergillus burnettii*. *ChemRxiv*. doi.org/10.33774/chemrxiv-2021-p016t

(37) Gilchrist, C. L. M., Lacey, H. J., Vuong, D., Pitt, J. I., Lange, L., Lacey, E., Pilgaard, B., Chooi, Y. H., and Piggott, A. M. (2020) Comprehensive chemotaxonomic and genomic profiling of a biosynthetically talented Australian fungus, *Aspergillus burnettii* sp. nov. *Fungal Genet. Biol. 143*, 103435.

(38) Jensen, N. B., Strucko, T., Kildegaard, K. R., David, F., Maury, J., Mortensen, U. H., Forster, J., Nielsen, J., and Borodina, I. (2014) EasyClone: Method for iterative chromosomal integration of multiple genes in *Saccharomyces cerevisiae*. *FEMS Yeast Res. 14*, 238–248.

(39) Vanegas, K. G., Jarczynska, Z. D., Strucko, T., and Mortensen, U. H. (2019) Cpf1 enables fast and efficient genome editing in *Aspergilli*. *Fungal Biol. Biotechnol. 6*, 6.

(40) Robellet, X., Oestreicher, N., Guitton, A., and Vélot, C. (2010) Gene silencing of transgenes inserted in the *Aspergillus nidulans alcM* and/or *alcS loci*. *Curr. Genet. 56*, 341–348.

(41) Van Leeuwe, T. M., Arentshorst, M., Ernst, T., Alazi, E., Punt, P. J., and Ram, A. F. J. (2019) Efficient marker free CRISPR/Cas9 genome editing for functional analysis of gene families in filamentous fungi. *Fungal Biol. Biotechnol. 6*, 13.

(42) Jarczynska, Z. D., Rendsvig, J. K. H., Pagels, N., Viana, V. R., Nødvig, C. S., Kirchner, F. H., Strucko, T., Nielsen, M. L., and Mortensen, U. H. (2020) DIVERSIFY – a fungal multi-species gene expression platform. *ACS Synth. Biol. 10*, 579–588.

(43) Axelrod, D. E., Gealt, M., and Pastushok, M. (1973) Gene control of developmental competence in *Aspergillus nidulans*. *Dev. Biol. 34*, 9–15.

(44) Adams, T. H., Wieser, J. K., and Yu, J.-H. (1998) Asexual sporulation in *Aspergillus nidulans*. *Microbiol. Mol. Biol. Rev. 62*, 545–545.

(45) Wang, F., Sethiya, P., Hu, X., Guo, S., Chen, Y., Li, A., Tan, K., and Wong, K. H. (2021) Transcription in fungal conidia before dormancy produces phenotypically variable conidia that maximize survival in different environments. *Nat. Microbiol. 6*, 1066–1081.

(46) Sarkari, P., Marx, H., Blumhoff, M. L., Mattanovich, D., Sauer, M., and Steiger, M. G. (2017) An efficient tool for metabolic pathway construction and gene integration for *Aspergillus niger*. *Bioresour. Technol. 245*, 1327–1333.

(47) De Lorenzo, V., Krasnogor, N., and Schmidt, M. (2021) For the sake of the Bioeconomy : define what a Synthetic Biology Chassis is ! *N. Biotechnol. 60*, 44–51.

(48) Fang, F., Salmon, K., Shen, M. W. Y., Aeling, K. A., Ito, E., Irwin, B., Tran, U. P. C., Hatfield, G. W., Da Silva, N. A., and Sandmeyer, S. (2011) A vector set for systematic metabolic engineering in *Saccharomyces cerevisiae*. *Yeast 28*, 123–136.

(49) Lim, F. Y., Sanchez, J. F., Wang, C. C. C., and Keller, N. P. (2012) Toward awakening cryptic secondary metabolite gene clusters in filamentous fungi. *Methods Enzymol. 517*, 303–324.